Role of soil pore structure in water infiltration and CO_2 exchange between the atmosphere and underground air in the vadose zone: a combined laboratory and field approach

C. Pla [1*]; S. Cuezva [2,3]; J. Martinez-Martinez [1]; A. Fernandez-Cortes [4,5]; E. Garcia-Anton [3]; N. Fusi [6]; G.B. Crosta [6]; J. Cuevas-Gonzalez [1]; J.C. Cañaveras [1]; S. Sanchez-Moral [3]; D. Benavente [1].

(1) Departamento de Ciencias de la Tierra y del Medio Ambiente, Universidad de Alicante, San Vicente del Raspeig, 03690 Alicante, Spain.

(2) Geomnia Natural Resources SLNE, 28006 Madrid, Spain

(3) Museo Nacional de Ciencias Naturales (CSIC), José Gutiérrez Abascal 2, 28006 Madrid, Spain.

(4) Department of Earth Sciences, Royal Holloway, University of London, Egham, Surrey TW20 0EX, UK.

(5) Departamento de Biología y Geología, Universidad de Almería, La Cañada de San Urbano, 04120 Almería, Spain.

(6) Dipartimento di Scienze dell'Ambiente e del Territorio e di Scienze della Terra, Università degli Studi Milano-Bicocca, 20126 Milano, Italy.

*Corresponding author: c.pla@ua.es

Departamento de Ciencias de la Tierra y del Medio Ambiente, Universidad de Alicante, San Vicente del Raspeig, 03690 Alicante, Spain. Telephone: +34965903400 ext. 2095.

Abstract

The soils above caves represent a membrane that regulates the connection between the underground environment and the outside atmosphere. In this study, soils from two different field sites (Cueva de Altamira and Cueva del Rull in Spain) are investigated. Field results are analysed and linked to laboratory tests. Several laboratory experiments are performed to quantify CO_2 diffusion coefficients and water infiltration rates in these soils under different degrees of soil water saturation and compaction.

Tests confirm that the grain size distribution, organic matter content, mineral composition and water content of soils affect gas transport through the soil pore network. Both field and lab results reveal that Altamira soil has a coarser texture and therefore has higher CO_2 diffusion coefficients, infiltration rates and hydraulic conductivity values than Rull soil. Rull soil contains a higher proportion of fine particles and organic matter, which explains the lower fluid transport coefficients.

When soils are near saturation, fluid transport does not depend on the physical properties of soil but depends on the soil water content. In this state, liquid transport regulates the available space within the soil pores, which leads to a reduction in the gaseous diffusion coefficient of the soil. After rainfall episodes, the connection between the exterior atmosphere and underground cavities is hindered due to a rise in the soil water content, which is responsible for the closure of the overlying membrane. This study demonstrates that soil-produced CO_2 reaches the underground atmosphere through diffusion processes that are controlled by the intrinsic properties of soil (porosity, grain size distribution, texture, mineralogy and organic matter content) and soil water content.

Key words

CO_2, soil gas diffusion, water content, underground cave, vadose zone.

1. Introduction

In recent years, worldwide concern with global climate change has caused more attention to be paid to the vadose zone atmosphere since it has been established as an important reservoir of CO_2 (Bourges et al., 2012; Fernandez-Cortes et al., 2015a; Serrano-Ortiz et al., 2010). Soil-derived CO_2, including that derived from roots and soil organic matter, rhizosphere respiration, heterotrophic microbial respiration and respiration by autotrophs (Kuzyakov, 2006), fills the porous systems of soils and bedrock. This CO_2 is partially emitted, and represents a major flux of C to the atmosphere (Jassal et al., 2005; Schlesinger and Andrews, 2000). Simultaneously, significant amounts of CO_2 migrate by diffusion into voids in the underlying rocks (Faimon et al., 2012), such as natural cavities. There, the gas is temporarily stored. Large amounts of CO_2 are exchanged between shallow vadose systems and the atmosphere. As a result, the subterranean atmospheres of karstic terrains can act either as sinks or sources of CO_2 at different times, due to degasification – ventilation processes (Bourges et al., 2001, 2006; Cuezva et al., 2011; Fernandez-Cortes et al., 2015b; Garcia-Anton et al., 2014a; Kowalczk and Froelich, 2010).

The surface soil layer plays a key role in all these processes (Cuezva et al., 2011). On the one hand, it is the responsible for the CO_2 production, which depends on weather conditions and soil physical, chemical and biological properties (Moitinho et al., 2015), such as organic matter content, abundance of microorganisms, type and density of vegetation, etc. On the other, soil constitutes the primary interface through which liquid and gas passes between the outside atmosphere and the underground environment. This fluid transfer (i.e., gas and liquid movement) occurs through the soil pore network and is affected by the physical properties of soil, such as density, texture, pore network, mineral composition and organic matter content, among others. In addition, fluid transfer is also regulated by the degree of moisture in soil, which in turn depends on the infiltration processes whereby water enters the soil and adds to the total soil moisture (Huang et al., 2013).

Diffusion is mainly responsible, combined with advection, for CO_2 transport from the soil (where it is produced) to these underground cavities, where it can be naturally stored (Garcia-Anton et al., 2014a). When CO_2 is transported through the soil pores, the presence of other fluids affects gas movement. CO_2 movement is strongly affected by soil water content, since liquid water reduces the air filled porosity and the connection between pores. The degree of saturation of the soil and, consequently, the gaseous transport of CO_2, varies in response to environmental conditions such as the amount and intensity of

rainfall, wetting – drying cycles (Alletto et al., 2015) and the degree of soil compaction (Kuncoro et al., 2014).

Characterization of the combined transport of CO_2 and water through the soil pore network is a challenging task. The presence of water is widely considered when estimating the rate of soil CO_2 production (Hashimoto and Komatsu, 2006; Phillips et al., 2011; Xu et al., 2004) as it is an essential factor. However, with regard to the diffusive gas transport through soils, available studies which combine both fluids (CO_2 and water) are scarce. Soil gas diffusion is frequently estimated using mathematical models derived from soil physical properties (Currie, 1960; Millington and Quirk, 1960; Moldrup et al., 1996; Penman, 1940; Troeh et al., 1982). Most of these models consider the water content of soil when calculating the diffusion coefficient, but unfortunately some of these models can only be used to estimate diffusion coefficients for a limited range of air-filled porosity values (Jabro et al., 2012).

Previous studies (Jabro et al., 2012; Turcu et al., 2005) have estimated the CO_2 diffusion coefficient in soils using laboratory and field tests. They obtained relevant information about CO_2 fluxes through natural soils. In addition, some of these studies confirmed that the variation of water content in soil influences soil CO_2 diffusion coefficients (Pingintha et al., 2010) and highlighted the importance of developing a deep understanding of the subject.

The main objective of this study is to assess the combined water and CO_2 transport among different reservoirs in the atmosphere-soil-cave system in two different natural scenarios. Special attention is given to the mineralogical, textural and physical properties of soils in order to demonstrate their role as a membrane that controls fluid exchange. To achieve this goal, new methodological procedures are implemented, including a specially designed system for measuring CO_2 diffusion and the use of X-ray Computed Radiography (X-ray CR) to observe the real behaviour of water movement through soils. CO_2 diffusion and water infiltration experiments are performed in soil samples with different water contents. The laboratory results are linked to field studies of the Altamira and Rull caves, including measurements of CO_2 fluxes, and isotopic analysis, as well as an examination of microclimatic and external weather conditions in different periods.

2. Site and Methodology

2.1. Study sites

Soils located above Altamira and Rull caves are studied. Both underground caves have important differences in geomorphology, microclimate, external weather conditions, soil and rock compositions, etc.

Altamira cave (43º 22' 40'' N; 4º 7' 6''W) is located in northern Spain (Cantabria province). It is a shallow vadose cavity characterized by remarkable stable environmental conditions (Cuezva et al., 2009; Saiz-Jimenez et al., 2011; Sanchez-Moral et al., 1999). The main entrance to the Altamira cave is secured by an insulated metal gate (slotted surface <4%), which acts as a barrier to stop the exchange of energy and matter with the outside. The cave is in the upper vadose zone of the karstic system. The cave lies at a depth of 3-22 m (8 m on average) below the surface, under a hill with an elevation of 161 m.a.s.l. The cave has a single entrance in a topographically elevated position (152 m.a.s.l.) and includes several main rooms that slope downward from the entrance to the deepest part of the cave. The rock layer over the chamber averages 7.5-8 m in thickness. The host rock of the Altamira cave is a thin- to medium-bedded, parallel-bedded, Cenomanian (Upper Cretaceous) limestone succession that ranges in thickness from 13.5 to 15 m. The soil above the cave is heterogeneous and includes artificial backfill, poorly differentiated. Originally, there was a thin, patchy soil profile partly covering the karstified bedroc. Extensive agricultural activity, mainly conditioning pastures for livestock, resulted in the current anthropogenic soil. This soil has little profile development (30 – 70 cm) and only a surface horizon A. It is a silty loam soil with a mineral composition dominated by quartz (Cuezva et al., 2011). A developed plant cover (meadow vegetation, C3 plants) and high organic carbon were derived from this soil. In this geographical area, the climate is moderately oceanic and humid, with an annual precipitation of approximately 1400 mm and a mean annual temperature and relative humidity of 14 ºC and 85%, respectively. Rain continuously influences the overlying soil. Cave air is characterized by a highly stable temperature and humidity throughout the year, with an indoor relative humidity permanently near saturation and mean annual temperature near 14 ºC, with 1.5 ºC annual thermal amplitude (Cuezva et al., 2009). Relatively high CO_2 levels of cave air are registered during winter, which sometimes exceed 5000 ppm. The lowest values (near 500 ppm) occur during summer (from June to October), due to the most effective cave ventilation in this warmer and drier

period (Kowalski et al., 2008; Sanchez-Moral et al., 1999). The spatial distribution of pCO_2-air along the cave is nearly homogeneous (Garcia-Anton et al., 2014b).

Rull cave (38º 48' 40"N; 0º 10' 38"W) is located in the south-eastern area of Spain (Alicante province). The cave is located in massive Miocene conglomerates characterized by considerable textural and petrophysical complexity (de Carvalho et al., 2013), which were deposited on Cretaceous limestones. The host rock is composed of oligomictic calcareous orthoconglomerates. Framework clasts mainly consist of limestones. The matrix between the pebble-size clasts shows variable texture and composition, ranging from micritic (with different grades of recrystrallization) to sand matrix, with limestone and terrigenous (mainly quartz) grains. Mosaic calcite cement predominates. Other types such as ferruginous or bioinduced micritic cements are also recognized. Primary porosity is mainly intergranular. Conduits and fissures are related to calcite dissolution.

The relative thickness of the overlying host rock varies from 9 to 23 metres. The soil above the cave has a thickness of about 1 m with coarse to fine texture and it is discontinuous along the cave surface. The soil is mainly composed by quartz, related to the presence of the conglomerates. The soil is classified as a silty – silty loam soil (Pla et al., 2016a). The only differentiated horizons are the O horizon (a thin soil layer dominated by organic matter) and the A horizon (a mineral horizon near surface with accumulation of humified organic matter mixed with the mineral fraction). The vegetation consists of C3 plants, which are distributed in the form of Mediterranean shrubs. Rull cave area is defined by a Mediterranean sub-humid climate (Rivas-Martinez, 1984). Opposite to Altamira area, mean value of annual precipitation in Rull cave (October 2012-November 2014) is 377 mm. The scarce precipitations and the high temperatures during summer (exceeding in some cases 38 ºC) are responsible for the lack of moisture in the soil above the cavity. Rull cave is characterized by a thermo-hygrometric stability even with the presence of visitors (an average annual value of 13270 people visit the cavity). The soil-cave system response to the external weather conditions is slower than in Altamira. The gas natural dynamics in the cavity is responsible for the CO_2 variations (Pla et al., 2016b). Concentration varies from 463 ppm in the coldest months to 4065 ppm in summer.

In each cavity the gas dynamics is different but both of them (Altamira and Rull caves) suffer an annual cycle characterized by two main stages. Throughout the outgassing stage the connexion between the underground and the outdoor atmosphere is active and the gas interchange is allowed. This means that

a ventilation process (temperature-driven air flow) is responsible for the CO_2 removal from the cavity (Breecker et al., 2012). On the contrary, in the isolation stage the gas interchange is limited. The soil-produced CO_2, which moves through it primarily by diffusion and finally reaches the cavity, originates an important increase in the CO_2 content of cave air**.** While Altamira cave remains ventilated during the summer season, Rull cave follows an opposite pattern, remaining ventilated in the winter season. In Altamira and Rull caves, relationships between cave and exterior temperatures and the density gradient between the air masses control the air exchange, temporally determined by their differences in the geomorphologic features.

In both caves, host rocks are low porous limestones and present interparticle and touching vuggy pores. Interparticle pore size is lower than 0.1 μm, while vuggy porosity (constituted by fractures, fissures and solution channels) has a fissure width larger than 500 μm (Cuezva et al., 2011; Pla et al., 2015).

2.2. Monitoring field procedures

Microclimatic conditions in both caves were monitored by means of the same commercial type of climatic recorders. Further information of the monitoring systems can be found in Cuezva et al., 2011, Garcia-Anton et al., 2014a and Pla et al., 2015. The monitoring station was composed of an 8-channel, 16-bit datalogger (COMBILOG TF 1020, Theodor Fiedrich & Co., Germany) with a suite of probes. Particularly, a non-dispersive infrared analyser (ITR 498, ADOS, Germany), 0-10000 ppm measurement range and 0.3% accuracy with a suction pump was used to measure CO_2 concentrations. The station scanned each sensor every 10 s and recorded the 15 min averages. Rainfall amount was registered in the exterior of Altamira and Rull caves by a 147 RG2-M rain gauge (Onset Computer Corporation, Bourne, MA, USA, resolution 0.2 mm). In both locations soil temperature was controlled by a HOBO U12 logger (Onset, Bourne, MA, USA, accuracy ±0.5 ^{o}C) whereas volumetric water content was measured with an ECHO EC-5 probe (Decagon Devices, USA, accuracy 1-2%).

Spot air sampling was also performed in both caves in order to characterize the spatial distributions and temporal variations of CO_2 concentration and its $\delta^{13}C$ signal. The sampling was conducted inside the caves, in the soil above them and in the exterior atmosphere. Soil air was pumped using an iron tube nailed to the ground by means of a micro-diaphragm gas pump (KNF Neuberger, Freiburg, Germany) at 3.1 l min^{-1} at atmospheric pressure. Exterior air and air from the caves was sampled with an air pump. Air was saved

in 1 l Tedlar bags with lock valves and then analysed in a period no longer than 48 h after sampling, using a Picarro G2101-i analyser (California, USA, accuracy of 0.3‰ for $\delta^{13}CO_2$ after 5 minutes of analysis) that employs cavity ring-down spectroscopy (CRDS-WS) (Crosson, 2008). The analyser measures the isotopologues of the carbon dioxide ($^{12}CO_2$ and $^{13}CO_2$) and automatically calculates the isotopic value, $\delta^{13}CO_2$. The field campaigns were carried out monthly or bimonthly. In Altamira, they were performed from September 2011 to September 2012. A total amount of 230 bags were analysed from the cavity (117), soil air (58) and exterior atmosphere (55). At Rull cave, field campaigns were monthly – bimonthly performed from January 2014 to May 2015. The number of analysed samples was 200 (96 from the cavity, 58 from soil air and 46 from exterior atmosphere).

In addition, an automated soil CO_2 flux system (Li-8100, Li-Cor, accuracy of 1.5% of CO_2 concentration reading) with Long-Term Chamber 8100-104 was employed to make continuous measurements of CO_2 flux in Rull field site. The field campaign was performed for a 2h period in January 13, 2014. The chamber was installed in the soil above the cave over a single PVC collar (20 cm inner diameter). The Long-Term Chamber was programmed to make measurements every 5 minutes for a period of 2 h, allowing aeration between measurements. Soil CO_2 fluxes were estimated using the initial slope of a fitted exponential curve adjusted for the total (chamber and collar) volume.

2.3. Laboratory characterization

2.3.1. Physical properties of the soil

Soil samples were collected from both study sites (Altamira and Rull caves) from a deep of 5 to 10 cm (below the main rooting zone) with steel rings (sampling volume of 21 cm^3). Some tests required undisturbed soil samples while others required treated samples. In these cases, the collected samples were lightly sieved and gravel and root debris were carefully removed in order to prepare them.

Grain size distribution for Altamira and Rull soil was obtained by sieving and laser granulometry (Malvern Mastersizer 2000). Two repetitions of the analysis were performed for each soil. Soils were oven dried at 40 ^oC for 24 h to determine the dry bulk density. Mineral phase identification was determined by powder X-ray diffraction (XRD) using a Philips PW diffractometer using Cu Kα radiation. Mineral characterization was performed to both randomly oriented powder samples. Soils were milled in an agate mortar to <40 μm particle size, and then analysed. XRD patterns of the randomly oriented powder were collected and

interpreted using the XPowder software package. The qualitative search-matching procedure was based on the ICDD-PDF2 database.

The grain density (particle or real density) was obtained using an AccuPyc 1330 Helium pycnometer. The total porosity was derived from grain and bulk densities (Tiab and Donaldson, 1996). The air-filled porosity was calculated as the difference between the total porosity and the soil water content. The determination of the specific surface area of the soil samples was accomplished by using the nitrogen absorption technique through the BET method (Rouquerol et al., 1994). Hydraulic tests were carried out in a triaxial device (Controls Triax 100) with an automatic pressure system using the steady-state method (Benavente et al., 2007; Galvan et al., 2014). Organic matter content was determined by the Walkley-Black method.

2.3.2. Soil CO_2 gaseous diffusion coefficient

The CO_2 gaseous diffusion coefficient for soils was measured in a specially designed laboratory system following the gradient method, very similar to those previously used in other studies (Albanito et al., 2009; Rolston and Moldrup, 2002; Turcu et al., 2005). The soil was placed in a sealed cell between two vertical differentiated chambers with identical volume (Fig. 1). A constant injection of CO_2 gas (2000 ppm) was performed in the bottom cell, so that the measured CO_2 in this chamber remained always constant for the whole procedure. A CO_2 probe (GMP222 Vaisala Carbocap) with a measurement range of 0-10000 ppm was installed in each chamber connected to a datalogger (CR-1000 Campbell Scientific). Temperature inside the chambers remains constant (20 ^{o}C) as well as the working pressure (atmospheric pressure). In the top chamber, the CO_2 concentration was maintained at 0 ppm at the beginning of the experiment. The diffusion process is well guaranteed due to the concentration gradient between the two chambers. The CO_2 diffusion coefficient was calculated recording the time taken for the top chamber to reach the equilibrium with the bottom chamber and using the model of Zhang et al. (2005), which assumes that gaseous flux across the soil achieves a steady-state flux even though the CO_2 concentrations in the chambers change with time. Two repetitions of the experiment in each sample were performed. When the CO_2 diffusion coefficient was obtained an average CO_2 flux was calculated for each experiment by applying the Fick´s law of diffusion.

To observe the changes in the diffusion coefficient and related to density and water content variations in soil, both soils were tested under different conditions. Soil samples from Rull and Altamira were tested

completely dry after oven dried (Rull 0% and Alt 0%), and with water contents of 30% (Rull 30% and Alt 30%) and 62% (Rull 62% and Alt 62%). In addition, a duplicate test was carried out with compacted samples for the dry soil (Rull 0% compacted and Alt 0% compacted). To prepare soil samples they were homogeneously mixed by adding different water amounts. Percentages were calculated as the ratio of total water mass / total soil mass. Samples were compacted by pushing the soil by hand with the help of a custom made piston. The compaction method tried to reproduce nearly the same porosity that the original soil. The compaction was identically performed in all the samples using the same pressure piston and recipients. In the wet samples, water was added to reach the same bulk density. Previous studies used similar procedures to prepare soil samples (Huang et al., 2013; Kuncoro et al., 2014; Menon et al., 2015, among others). Bulk densities after water addition were around 1.3 – 1.4 g cm^{-3} in all the samples from Rull and Altamira, being hardly less dense the drier samples. The compacted samples from Rull and Altamira had bulk densities up to 1.13 times bigger than the non-compacted samples.

2.3.3. Water flux characterization

A high resolution X-ray Computed Radiography (BIR Actis 130/150) was used to characterize the liquid movement of water through the studied samples. X-ray CR scanners have been proved an effective tool to investigate the internal structure of materials and different processes without disturbance (Ketcham and Carlson, 2001). Samples for this study were prepared in a soil core sampler (9.5 cm^3 in volume) and placed in the scanner between the X-ray generator and detector. An initial radiography was obtained by means of a 12-bit digital camera which collects light radiations in raw data and sends them to the computer, where they are processed as black – white images (radiographies, DR) (Fusi and Martinez-Martinez, 2013). After that, a 4 ml drop of KI tracer (15% dissolution) was carefully deposited in the soil surface with a syringe. In order to achieve sufficient density contrast between fluid and matrix, the concentration of KI in the injected solution was carefully defined. A new DR was captured every 2 minutes (minimum time gap forced by the apparatus design) during the first 20 minutes. After that, the capturing interval became higher. The experiment comprised a total period of 1.5 h and a sequence composed by 20 pictures. The consecutive radiographies show the progression of the infiltration front through the soil profile.

A vertical grey level profile was obtained from each DR by means of digital image analysis (Fig. 2(a)). The

profile was drawn in the centre of the sample using the open source software Jmicrovision v.1.2.7. (Roduit, 2015). Grey level scale ranged from 0 (black tones, tracer) to 250 (white tones, pure air). Vertical axis of these profiles corresponds to distance (pixels, then converted to meters). A characteristic step in this kind of profile is observed corresponding to the change from the wet (dark) to the dry (light) part of the soil. The different position of this step between two consecutive DR is consequence of the water progress through the soil. The infiltration rate (m s^{-1}) was calculated measuring this distance divided by the time lapse.

Two different infiltration rates were obtained: the initial and the total rate (R_i and R_t, respectively). Initial rate quantifies the fast water percolation carried out during the first 2 minutes of the test. It is calculated by comparing the grey level differences between the image 1 and 2 of the sequence. The total rate shows the maximum depth reached by the drop during the test and it is calculated with the profiles of the images 2 and 20.

This methodology was applied to 10 different soils: 6 of them from Altamira and 4 from Rull. Each soil sample was prepared in order to obtain different water contents. The procedure was exactly the same than the procedure followed in the diffusion experiment. In this test both soils (Rull and Altamira) were tested completely dry, after oven dried, and with water contents of 22, 30, and 62%. Two samples from Altamira (Alt 0% and Alt 30%) were also tested after compaction (Alt 0% compacted and Alt 30% compacted).

2.3.4. Relative hydraulic conductivity as a function of water volume content in the soil (ku-pF apparatus)

Hydraulic conductivity as a function of water volume content was obtained for Altamira and Rull soil samples. The test was carried out in ku-pF Apparatus DT 04-01 (UGT, Germany). Soil samples (fully saturated) were introduced in a sample ring, sealed at the base. During the test, the free surface of the ring was exposed to evaporation. The gradient of the water movement (amount of water that passes through the sample surface) was measured by weighting. The gradient of water tension was measured with two tensiometers spaced at a distance of 3 cm into the sample ring. The hydraulic conductivity of the soil samples was calculated according to Darcy´s equation, assuming quasi-stationary flow. The hydraulic gradient in the sample ring was always constant throughout the sample height. The gradient was calculated from the matric potential (tensiometer measurement) and the gravitational potential. Due

to evaporation, a flow rate occurred at the free sample surface. Basal sealing established a flow rate = 0 at the bottom of the sample.

3. Results and Discussion

3.1. Field results

3.1.1. CO_2 and δ^{13} CO_2 in air samples

Spot air sampling in both caves was essential to identify the CO_2 source. Stable isotopes are a powerful tool for identifying autotrophic and heterotrophic respiration in soils ($\delta^{13}CO_2$) (Bahn et al., 2012). When drawing a "Keeling plot" for the analysis of $\delta^{13}CO_2$ isotopic signals (Keeling, 1958), the model determines, by a linear regression approach, the carbon isotopic signal of the CO_2 sources of a specific ecosystem that contributed to increases in atmospheric CO_2. According to this method, the CO_2 concentration in the cave air is the result of mixing of background atmospheric CO_2 with soil-produced CO_2. The different components in the both caves show a high degree of correlation (R^2 = 0.98 for Altamira and 0.95 for Rull) when fitting the annual data to the Keeling model (Fig. 3(a, b)). Samples of cave air are close to soil air values but less similar to exterior air. In addition, the y-intercept values for Altamira (-27.74‰) and Rull (-27.58‰) indicate that a dominant component of soil organic CO_2 originated from soil organic respiration in both cases (Garcia-Anton et al., 2014a). The $\delta^{13}CO_2$ of approximately −27‰ is the result of the combination of equilibrium and kinetic fractionations that occur during the photosynthesis of C3 plants and the decomposition of C3 biomass (Amundson et al., 1998; Cerling et al., 1991). In both caves, the $\delta^{13}CO_2$ isotopic signal fluctuates cyclically, and this behaviour is linked to gas dynamics (Garcia-Anton et al., 2014a; Pla et al., 2016a; Sanchez-Moral et al., 2010). Particularly for Rull cave, the heavier $\delta^{13}CO_2$ values are caused by the strong influence of the external atmosphere, which is most pronounced during the degassing stage (i.e., during the coldest months). Lighter values of $\delta^{13}CO_2$ in the cave indicate that soil-produced CO_2 dominates, as occurs in the recharge stage during the warmest months (Pla et al., 2016a).

Abiotic reactions can also control the CO_2 exchange between air, water, soil and host rock. The CO_2 generated by carbonate dissolution and subsequent degassing associated with calcite precipitation might flow from the soil and epikarst to the cave. Breecker et al. (2012) concluded that soil-derived (biotic) CO_2

constitutes the main CO_2 source in cave atmospheres. Thus, the contribution of abiotic CO_2 is negligible compared to the organic CO_2, which agrees with the low rates of dripping water observed in the cave during the study.

3.1.2. CO_2 flux campaign

CO_2 fluxes were measured directly in the soil above Rull cave. While performing the field flux campaign it started raining. Before the rain, large positive fluxes were measured when the volumetric water content in soil (VWC) reached the lowest observed values (Fig. 4(a)). CO_2 fluxes varied from 1.8 to 2.3 µmol m^{-2} s^{-1}, while VWC values ranged from 0.063 to 0.071 m^3 m^{-3}. When the water content in soil decreases, CO_2 flux through soil is enhanced. Average soil temperature for this period was 9.55 °C with variations less than ± 1 °C. These relatively constant temperatures resulted in similarly constant CO_2 production rates and diffusivities during the studied event. CO_2 flux in soil is driven primarily by the CO_2 diffusion gradient. Consequently, soil CO_2 flux is described by the CO_2 diffusion coefficient. Although the CO_2 production rate and diffusivity in soil are controlled by several variables, the results show a clear relationship between the measured CO_2 flux and the soil water content. A negative correlation (R^2 = 0.90) was found when performing a linear regression analysis between the CO_2 flux and the soil VWC, which illustrates the influence of soil water content on CO_2 diffusivity (Fig. 4(b)).

3.1.3. Relationships between soil water content and the CO_2 content of cave air

The relationship between the gaseous concentration inside both caves and soil water content was analysed during brief periods after rainfall episodes. These periods occurred during the outgassing stage of each cave, when air renewal due to cave ventilation is more active and lower CO_2 concentrations are registered inside the caves. The effects of the VWC increase in soils are highlighted when studying changes in the CO_2 content of cave air.

Data from the Altamira cave were collected during September 13 to 26, 2009 (Fig. 5(a)). During this period, the total amount of rainfall was 114.2 mm. Volumetric water content (VWC) in the soil increased from 0.4 m^3 m^{-3} (before the rainfall) to nearly 0.9 after the first water contribution to soil, and remained at very high levels during days when rain fell constantly. No visitors could access to the cave during this episode. Thus, the cave was under totally natural conditions. Immediately after the first rainfall episode, a CO_2 concentration increase (from 1065 to 2008 ppm in 48 h) was observed inside the cave. When the rainfall

episode started, the soil needed very little time to become saturated since it already contained a considerable amount of water. Therefore, water transport began quickly (Fig. 5(a)).

Precipitation is scarce near the Rull cave, but from March 18 to 24, 2015, rain fell continuously, totalling 180.4 mm (Fig. 5(b)). Before the rainfall event, the soil was almost completely dry (0.14 m^3 m^{-3} VWC), a common situation in this study area. CO_2 concentrations inside the cave (950 ppm) were decreasing due to the ongoing outgassing stage, which is associated with the open connexion between the subterranean and outside atmospheres. Although Rull cave is open to the public, the effects of even a large number of visitors when they occur for several continuous days only persist for a few days during the outgassing stage (Pla et al., 2016b). Thus, the presence of visitors during the study period may not have affected microclimatic conditions within the cave.

On March 18, in response to the rainfall episode, soil VWC changed (from 0.14 to 0.20 m^3 m^{-3}) (Fig. 5(b)). In the following days, the amount of water in soil was substantially higher than the mean annual value due to the continuous influx of water, which also affected the soil temperature. The last and most significant rainfall (51.8 mm) occurred on March 24. This was the main rainfall event responsible for the large observed increase in soil VWC (0.25 m^3 m^{-3}). After this event, CO_2 concentration inside the cave increased from March 24 to March 29. Under other circumstances, i.e., without rain, the natural CO_2 trend inside the cave would have decreased during this period (Pla et al., 2016a, 2016b). During the studied event, the role of carbonate host rock dissolution as a contributing source of CO_2 to the cave air (Serrano-Ortiz et al., 2010) is considered to be negligible because little water was observed dripping into the cave after the rainfall event.

Isotopic sampling was not performed after the rainfall episode. However, previous studies that examined the annual isotopic cycle (Pla et al., 2016a) have shown that $\delta^{13}CO_2$ values in Rull cave become lighter after the rainfall event. Cave $\delta^{13}CO_2$ measured values were -17.80‰ (16/02/2015) and -23.57‰ (15/04/2015). Large numbers of visitors entered the cave on March 28 and 29, which might also have contributed to the registered CO_2 concentration increment.

The highest CO_2 concentration observed as a direct consequence of the rainfall was achieved between March 28 and 29, some days after the last rainfall on March 24. After this last episode, soil VWC started decreasing but always remained higher than the value observed before the first rainfall episode (March 18).

Soil production of CO_2 is strongly influenced by soil temperature (Darenova et al., 2014; Li et al., 2015). However, CO_2 fluxes increase after rainfall events. This effect is more pronounced after dry periods without precipitation (Xu and Luo, 2012), which produce a large CO_2 concentration gradient between soil and cave, accentuating the CO_2 diffusion process. The average soil CO_2 content is higher at Altamira (2773 ppm, September 2011 – September 2012) than at Rull (1828 ppm, January 2014 – May 2015). The differences between the evolution in gas dynamics in both caves are shown in Fig. 5(a, b). The observed CO_2 increase (1000 ppm) in Altamira cave occurred abruptly in the hours following the rainfall event. At Rull cave, a small increase in CO_2 concentrations (200 ppm) was registered more than 48 h after than the first rainfall (March 18), when the saturation in soil was noticeable. The largest increase (600 ppm) did not appear until 48 h after the last rainfall event (March 24), and this rise was superimposed on a gradual increase.

Cuezva et al. (2011) confirmed that, at Altamira cave, the soil acts as a barrier or membrane which controls gas exchange between cave and atmosphere. This barrier becomes more or less effective as the amount of water in the soil pore system changes. At Rull cave, soil saturation is not accomplished immediately after rainfall events. This delay prevents total closure of the soil membrane above the cave, allowing gas transport to continue for several days after the beginning of the rainfall event. After the rainfall episode, the soil returns to lower water content levels and the connection between exterior atmosphere and soil is restored.

The rock properties of both caves also control the cave – atmosphere connection. Fluid transport is accomplished through the secondary porosity, including fractures, fissures and solution channels. Water flow is easily accomplished from the soil to the cave. However, gas transport depends on the degree of saturation of secondary porosity-related openings. Several factors, such as the thickness of the overlying membrane, as well as the characteristics of the karst geomorphology and the host rock, also influence the water and gas dynamics.

3.2. Physical properties of the soil

The grain size distributions for both soils are: <0.002 mm (1.1%), 0.063 – 0.002 mm (62.5%), 2 – 0.063 mm (36.4%) for Altamira soil and <0.002 mm (2.2%), 0.063 – 0.002 mm (80.1%), 2 – 0.063 mm (17.7%) for Rull soil. In other words, Rull soil has more fine particles than Altamira soil. XRD analysis of randomly-oriented

powder samples shows predominantly quartz in both soils, although Rull soil contains a greater proportion of phyllosilicates, as well as some calcite. Rull soil is composed of quartz (70%), phyllosilicates (20%), calcite (5%) and feldspars (5%). Altamira soil is composed of quartz (85%), phyllosilicates (12%) and feldspars (3%). Rull soil displays lower grain density values, due mainly to the presence of phyllosilicates, which have low specific gravities.

Porosity values for the two soils are similar but the higher water content in Altamira soil when the samples were taken leads to higher values of air-filled porosity for Rull samples (Table 1). For the experiments, sample preparation was designed to preserve the undisturbed soil texture. Thus, even considering possible variations between the original soil and the prepared samples, the lab experiments should be representative of processes that operate at the field sites.

Values of specific surface area (SSA) and organic matter content are higher in Rull soil than in Altamira soil, as consequence of the presence of fine particles in Rull soil. The amount and type of organic material are directly related to soil water repellency (hydrophobicity) (Neris et al., 2013), a phenomenon that prohibits water from wetting or infiltrating into dry soil. A hydrophobic soil can resist wetting for periods ranging from a few seconds to days or even months. Hydrophobicity also affects water affinity and, consequently, the soil's resistance to microbial degradation, the rate of wetting and absorption processes (Leelamanie, 2014). Nevertheless, some soils become hydrophilic with widely varying granulometric compositions and organic matter types (Vogelmann et al., 2013). When the organic matter is hydrophilic, the soil is able to hold large amounts of water. Under this situation, water absorption rates increase, resulting in more water being immobilized by the soil structure.

The SSA of polymodal porous materials is directly related to porosity and inversely related to pore size (Benavente et al., 2008). Thus, a sandy soil presents large pores, whereas clay soil contains narrow pores. In addition, the presence of clay minerals strongly increases SSA values since these minerals may have internal surfaces in their interlayer space. The higher specific surface area for Rull soil is consistent with its higher organic matter content (Table 1). The sample preparation prior to SSA measurement causes the removal of part of the organic matter. After this removal, SSA becomes higher. Initially, the narrowest pores are partially filled with organic matter, but after removal of the organic matter, this pore fraction becomes empty and, the SSA value increases (Ding et al., 2013; Kaiser and Guggenberger, 2003; Zhang et al., 2013).

3.3. CO_2 gaseous diffusion coefficient

CO_2 diffusion coefficients (Table 2) were determined for the samples at different degrees of compaction (Rull 0%, Rull 0% compacted, Rull 30%, Rull 62%, Alt 0%, Alt 0% compacted, Alt 30% and Alt 62%). Average values of CO_2 flux for the different experiments ranged from 0.71 to 8.96 µmol $m^{-2}s^{-1}$ in Altamira soils and from 0.71 to 3.32 µmol $m^{-2}s^{-1}$ in Rull soils, in relation to the CO_2 gaseous diffusion coefficients.

Figure 6 shows the CO_2 concentration as a function of time inside the top chamber for every sample. The CO_2 diffusion coefficients were obtained from these curves. These coefficients are in agreement with those obtained by previous studies (Jabro et al., 2012; Tang et al., 2003; Turcu et al., 2005).

Both samples (Altamira and Rull soils) were tested when partially and nearly totally saturated. Diffusion coefficients for Altamira soils are twice as large as for Rull soils, even when compacted. When the amount of water in soil increases, liquid transport regulates the available space within the soil pores. Significant reductions in the diffusion coefficient were found in comparison with the dry soil, which confirmed the influence of water content on gas diffusion. The final values of the diffusion coefficients for the partially and totally saturated samples are similar. Consequently, water content may be more important than pore structure. Both soils, Altamira and Rull, tend to homogenize their behaviour in the presence of water although they have different characteristics.

For both soils (Altamira and Rull), the differences between diffusion coefficients of dry and saturated samples are much higher than differences obtained between samples with different degrees of saturation (30 and 62% of water content). The CO_2 diffusion coefficients obtained for the totally dry samples (0%) were 5 times (for Rull soils) and 9 times (for Altamira soils) higher than those obtained from the saturated samples (62% water content). Figure 6 confirms that a decrease in soil water content enhances gas diffusion through the empty pores. As demonstrated previously by other authors (e.g., Fang and Moncrieff, 1998; Loisy et al., 2013; Sanci et al., 2009), increasing water content in soils produces a decrease in air-filled porosity, causing a reduction in CO_2 flux through the soil.

Classical diffusion models use equations in which soil porosity and water content are essential for determining the gaseous diffusion coefficient (Millington and Quirk, 1961; Penman, 1940). Nevertheless, the performed tests revealed that CO_2 diffusion coefficients for Altamira soils are larger than for Rull soils (Table 2), even though the porosity for Altamira soil is lower than that of Rull soil. This result confirms that

soil granulometry (which is coarser in Altamira soil than in Rull soil) may be decisive in determining gas fluxes through soil. Thus, sandy soils have higher gas diffusion coefficients than clay-rich soils, since the former have larger pores. For example, the clay fraction is included in the relative gas diffusivity, D/D_0, through empirical-determined coefficients (Ridgwell et al., 1999). The generally coarser particles in Altamira soil enhance gas diffusion through its pores. In contrast, the higher porosity values in Rull soil seem to be less decisive in the diffusion process than particle size distribution. Ridgwell et al. (1999) and Troeh et al. (1982), among other workers, developed diffusion models that specifically consider not only porosity and water content but also other soil physical properties. These models of gas diffusion indirectly consider total porosity and its reduction by increases in water content, and in the last instance, soil texture and organic matter content. In particular, the presence of organic matter affects gas diffusion through soil because it is a colloid that can modify soil texture and structure.

3.4. Infiltration rates determined by X-ray Computed Radiography

Results from X-ray CR reveal that, for all studied cases, the initial infiltration rates (R_i) (m s^{-1}) (Fig. 7(a)) are higher than the total rates (R_T) (Fig. 7(b)). This decrease in the water infiltration velocity might be related to one of two possible causes. (1) The tracer liquid was taken up in the superficial soil volume, occupying its voids. Consequently, no fluid remained to wet the remainder of the soil volume. In that case, the soil would have been partially saturated, with some pores completely filled with all the available water, and the moisture front would have stopped advancing through the soil. This hypothesis may explain the observed drastic reduction in the rate of moisture front advance during the last time intervals of the test, which was seen in results from practically all the samples. Moreover, liquid condensation – evaporation in the water islands formed between the pores, where the soil is wet, would encourage the transport of condensable vapour (Shahraeeni and Or, 2012). Alternatively, the decrease in the infiltration rate might be related to (2) the trapping of air during the initial saturation of the soil, as described by Faybishenko (1995). Initially, air accumulates in the smaller pores. When the infiltration process begins, water is absorbed into the smaller pores, displacing the entrapped air into the larger ones. Consequently, the largest pores are blocked, and the rate of liquid movement decreases. Unfortunately, the resolution of the experiment did not allow detection of changes in the soil porosity during testing, as these changes were not identified in the black-white radiographies (DR). Although not observed in our experiments, if

the flux of water entering into the soil had been constant, the entrapped air would have eventually been expelled in pulses.

For both soils tested, the infiltration front moves faster when the soil is completely dry. For the samples with 22, 30 and 62% water content, the infiltration front has lower rates of movement compared to the dry soil (Fig. 2(b, c)). In these samples, once the water content increased, the reduction in pores that were available to contribute to water movement caused lower infiltration rates. In Fig. 2(b, c), drier soils show lighter tones and lower densities.

Regarding the study areas, some differences are found between the soils from Rull and Altamira caves. Figure 7(a, b) shows the infiltration calculated rates, which are higher in Altamira soils for all tested water contents (0, 22, 30 and 62%). Initial infiltration rates (R_i) range from $2.06 \cdot 10^{-6}$ m s^{-1} to $1.42 \cdot 10^{-5}$ m s^{-1}. The decrease in the infiltration rate follows a constant slope for soils with 0 – 30% water content. Between 30 and 62% water content, the curve shows a significant change in slope. In Rull soils, infiltration rates are lower, ranging from $1.28 \cdot 10^{-6}$ m s^{-1} to $6.35 \cdot 10^{-6}$ m s^{-1}.

Regarding total infiltration rates (R_t), the infiltration front describes a similar pattern for both soils but net velocities are much lower, as described above. Observed differences between soils are consequences of their differing physical properties (Table 1), which was demonstrated by the different tests that were performed.

Two compacted samples from Altamira (Alt 0% compacted and Alt 30% compacted) were also tested. Coherent results were obtained (Figs. 2(b, c) and 7(a, b)) since infiltration rates were always smaller than those obtained from the non-compacted samples. In the non-compacted samples, velocity channels are available and the water flows easily. When soil compaction increases, pores decrease in size and become disconnected from each other (Menon et al., 2015), resulting in reduced water transport.

The infiltration front in Fig. 2(b, c) describes a curved shape in the less dense samples (Alt 0%, Alt 22%, Rull 0%). Infiltration took place primarily in the core of the soil sample. In these samples, no increase in the width of the soil border was detected in the top surface of the soil, as confirmed by the constant white band (air) that remained in the DR for the whole procedure. In contrast, compacted samples and samples with higher water contents were characterized by a planar and nearly immobile infiltration front that remained constant throughout the experiment. This planar infiltration front results in an increase in the width of the soil border in some samples (Alt 30% compacted, Alt 62%, Rull 30% and Rull 62%) because

the tracer was less able to percolate into the soil. As the liquid was not able to migrate downward, the water remained accumulated in the soil surface

3.5. Relative hydraulic conductivity as a function of soil water content

The relative hydraulic conductivity function was experimentally obtained for both soils (Fig. 8). The curves show that hydraulic conductivity of the unsaturated soils is not constant. It is predominantly a function of the water content or the matric suction of the unsaturated soils.

Figure 8 shows that the relative hydraulic conductivity of the soils decreases with decreasing soil water content. When the soil becomes unsaturated, air replaces some of the water in the larger pores. This replacement causes the water to flow through the smaller pores, leading to increased tortuosity of flow paths (Gallage et al., 2013). Water flux in soil is negligible at the lowest water contents, causing lower relative hydraulic conductivity values and higher water suction. In contrast, gas movement follows the opposite trend; when the water content in soil decreases, the CO_2 diffusion coefficient increases, as demonstrated by Fig. 8.

For any volumetric water content, the curve for Altamira soil shows larger values of relative hydraulic conductivity than the curve for Rull soil. This situation occurs because Altamira soil has a coarser grain size distribution, a large amount of void space and a lower organic matter content. Higher organic matter contents may be responsible for the observed water immobilization, which leads to lower values of the hydraulic conductivity. This effect was previously confirmed by Zongping et al. (2016) and Neris et al. (2012), who reported that soil infiltration and soil hydraulic conductivity were significantly affected by soil aggregation, structural stability, organic matter and bulk density. Hydraulic conductivity is a pore-space property and therefore depends on the connected porosity and pore size but also on textural properties such as grain shape, sorting and the internal grain arrangement of the material. Hydraulic conductivity is proportional pore size raised to some power (≈2), according to the Carman-Kozeny equation (Schön, 2011).

Hydraulic conductivity values measured under saturated conditions (Table 1) follow the same pattern as those measured under unsaturated conditions. Higher values of relative hydraulic conductivity encourage the downward flow of water into the soil subsurface during rainfall periods after the water content of the

soil increases. Relative hydraulic conductivity increases abruptly once the pore space is completely filled with water. Meanwhile, the soil becomes impermeable to gas transport.

3.6. Comparison of results: differences between Altamira and Rull caves

This study aims to establish the essential role of soil as one of the main controls on the gas exchange between underground environments and the outside atmosphere. Soil-produced CO_2 is transported mainly by diffusion through the soil-rock interface to the cavities (Garcia-Anton et al., 2014a, Pla et al., 2014). This soil-rock membrane regulates the gas exchange between the cave and the exterior, controlled by the soil's texture and water content (Fig. 9). The results obtained from the laboratory tests of Altamira and Rull soils show that they behave differently when fluids move through them. Altamira soil responds faster to fluid transport, and has higher infiltration rates, hydraulic conductivity values and gaseous diffusion coefficients than Rull soil. Altamira soil has higher bulk and grain densities, lower porosity, a coarser grain size distribution and lower organic matter content than Rull soil (Fig. 9). The soil mineral composition and organic matter content were found to be the essential factors that determine the ease of fluid transport. In Rull soil the attractive forces between the particles (which are generally finer than in Altamira soil) are responsible for the interaction between organic matter and clay minerals (Dikinya et al., 2008), reducing the filtration and diffusion paths in soil. The higher SSA value for this soil, which is a consequence of its texture, mineral composition and organic content, is responsible for its lower infiltration rates, hydraulic conductivity and gaseous diffusion coefficient.

At Rull cave, rainfall is scarce throughout the year, and the soil remains dry for long periods. After the observed rainfall episode in Rull cave (Fig. 5(b)), the CO_2 concentration increase did not occur simultaneously with the increase in soil moisture content (Fig. 9). The delay between these processes is a consequence of the low water infiltration rates and hydraulic conductivity values of Rull soil. In contrast, Altamira soil usually contains significant amounts of water, due to the abundant rainfall in the area (Fig. 9). At the beginning of the rainfall episode in Altamira cave (Fig. 5(a)), the effective rainfall (i.e., excess water left over after evapotranspiration) starts to percolate into the soil profile. The soil achieves higher water content values quickly, due to its high infiltration rates and hydraulic conductivity values. Once the soil membrane becomes fully saturated with water, a reduction in the gas diffusion from soil to cave air is evidenced in both caves by an increase in CO_2 concentrations. Altamira and Rull caves have a particular

pattern of gas exchange, controlled by the permeable-impermeable membrane formed by the host rock and soil.

4. Conclusions

The soils above Altamira and Rull caves have been demonstrated to be one of the main controls on the caves' gas dynamics. Although the two caves have different characteristics, similar processes having to do with the properties of the overlying soil control the migration of soil-produced CO_2 into the caves' underground atmospheres. This overlying soil, conforms, with host rock a permeable – impermeable barrier or membrane.

Experimental lab tests demonstrated that Altamira soil responds more quickly to fluid transport. Altamira soil, which has generally coarser particles than Rull soil, also has higher CO_2 diffusion coefficients, infiltration rates and hydraulic conductivity values. Rull soil is distinguished by finer particles, a mineral composition that includes larger amounts of clay and organic matter, which results in reduced rates of water filtration and gas diffusion. This fact explains the lower water transport coefficient and highlights the role of the soil mineral composition and organic matter content in fluid transport.

When both soils are dry, gas transport mainly depends on soil physical properties. Altamira soil, which has a higher gaseous diffusion coefficient, permits faster transfer of gases from the subterranean environment to the surface. When the water content in soil increases, the increased amount of available liquid regulates the available space within the soil pores, which leads to a reduction in the gaseous diffusion coefficient. For that reason, when both soils (Altamira and Rull) are near saturation, gas transport does not depend on the physical properties of the soil but on the water content.

After a rainfall episode, a rise in the soil water content closes off the soil-rock membrane above the cave, which hinders the connection between the exterior atmosphere and the cave. This consequence favours the diffusion of soil-produced CO_2 to the cave, which occurs when the soil-cave concentration gradient is large enough to drive diffusion. This process is controlled by soil properties, including porosity, granulometry, texture, mineralogy and organic matter content and soil water content.

Acknowledgements

This research was funded by the Spanish Ministry of Economy and Competitiveness projects CGL2011-25162 and CGL2013-43324-R and its programme Torres Quevedo (PTQ 13-06296). A pre-doctoral

research fellowship (BES-2012-053468) was awarded to C. Pla for the project CGL2011-25162. Funding was also provided by the People Programme (Marie Curie Actions – Intra-European Fellowships, call 2013) of the European Union's Seventh Framework Programme (FP7/2007-2013) under the REA grant agreement nº 624204. The authors thank cave managers for their collaboration throughout the entire investigation. We also thank to Dr. M. Cerdán for her inestimable help in the determination of the soil organic matter content and F. Tárraga and all the members of the UA electronic lab and J.M. Martínez for their valuable technical support.

References

Albanito, F., Saunders, M., Jones, M.B., 2009. Automated diffusion chambers to monitor diurnal and seasonal dynamics of the soil CO_2 concentration profile. Eur. J. Soil Sci. 60(4), 507-514. http://dx.doi.org/10.1111/j.1365-2389.2009.01154.x.

Alletto, L., Pot, V., Giuliano, S., Costes, M., Perdrieux, F., Justes, E., 2015. Temporal variation in soil physical properties improves the water dynamics modeling in a conventionally-tilled soil. Geoderma 243–244(0), 18-28. http://dx.doi.org/10.1016/j.geoderma.2014.12.006.

Amundson, R., Stern, L., Baisden, T., Wang, Y., 1998. The isotopic composition of soil and soil-respired CO_2. Geoderma 82(1–3), 83-114. http://dx.doi.org/10.1016/S0016-7061(97)00098-0.

Bahn, M., Buchmann, N., Knohl, A., 2012. Stable isotopes and biogeochemical cycles in terrestrial ecosystems. Preface. Biogeosci. 9(10), 3979-3981. http://dx.doi.org/10.5194/bg-9-3979-2012.

Benavente, D., Cueto, N., Martinez-Martinez, J., Garcia-del-Cura, M.A., Cañaveras J.C., 2007. The influence of petrophysical properties on the salt weathering of porous building rocks. Environ. Geol. 52, 197–206. http://dx.doi.org/10.1007/s00254-006-0475-y.

Benavente, D., Cultrone, G., Gomez-Heras, M., 2008. The combined influence of mineralogical, hygric and thermal properties on the durability of porous building stones. Eur. J. Mineral. 20(4), 673-685. http://dx.doi.org/10.1127/0935-1221/2008/0020-1850.

Bourges, F., Mangin, A., d'Hulst, D., 2001. Carbon dioxide in karst cavity atmosphere dynamics: the example of the Aven d'Orgnac (Ardeche). C.R. Acad. Sci., Ser. IIa: Sci. Terre Planets 333(11), 685-692. http://dx.doi.org/10.1016/s1251-8050(01)01682-2.

Bourges, F., Genthon, P., Mangin, A., D'Hulst, D., 2006. Microclimates of l'Aven d'Orgnac and other French limestone caves (Chauvet, Esparros, Marsoulas). Int. J. Climatol. 26(12), 1651-1670. http://dx.doi.org/10.1002/joc.1327.

Bourges, F., Genthon, P., Genty, D., Mangin, A., D'Hulst, D., 2012. Comment on Carbon uptake by karsts in the Houzhai Basin, southwest China by Junhua Yan et al. J. Geophys. 117, G03006. http://dx.doi.org/10.1029/2012JG001937.

Breecker, D.O., Payne, A.E., Quade, J., Banner, J.L., Ball, C.E., Meyer, K.W., Cowan, B.D., 2012. The sources and sinks of CO_2 in caves under mixed woodland and grassland vegetation. Geochim. Cosmochim. Ac. 96, 230-246. http://dx.doi.org/10.1016/j.gca.2012.08.023.

Cerling, T.E., Solomon, D.K., Quade, J., Bowman, J.R., 1991. On the isotopic composition of carbon in soil carbon-dioxide. Geochim. Cosmochim. Acta 55(11), 3403-3405. http://dx.doi.org/10.1016/0016-7037(91)90498-t.

Crosson, E.R., 2008. A cavity ring-down analyzer for measuring atmospheric levels of methane, carbon dioxide, and water vapor. Appl. Phys. B Lasers Opt. 92, 403–408. http://dx.doi.org/10.1007/s00340-008-3135-y.

Cuezva, S., Sanchez-Moral, S., Saiz-Jimenez, C., Cañaveras, J.C., 2009. Microbial communities and associated mineral fabrics in Altamira Cave, Spain. Int. J. of Spel. 38(1), 83-92.

Cuezva, S., Fernandez-Cortes, A., Benavente, D., Serrano-Ortiz, R., Kowalski, A.S., Sanchez-Moral, S., 2011. Short-term CO_2(g) exchange between a shallow karstic cavity and the external atmosphere during summer: Role of the surface soil layer. Atmos. Environ. 45(7), 1418-1427. http://dx.doi.org/10.1016/j.atmosenv.2010.12.023.

Currie, J.A., 1960. Gaseous diffusion in porous media Part 1. A non-steady state method. Br. J. Appl. Phys. 11(8), 314-317.

Darenova, E., Pavelka, M., Acosta, M., 2014. Diurnal deviations in the relationship between CO_2 efflux and temperature: A case study. Catena 123, 263-269. http://dx.doi.org/10.1016/j.catena.2014.08.008.

de Carvalho, L., Pla, C., Galvan, S., Cuevas-Gonzalez, J., Andreu, J.M., Cañaveras, J.C., Benavente, D., 2013. Caracterización petrográfica y petrofísica de la roca encajante de la Cueva del Rull (Vall d'Ebo, Alicante). Macla 17, 39-40.

Dikinya, O., Hinz, C., Aylmore, G., 2008. Decrease in hydraulic conductivity and particle release associated with self-filtration in saturated soil columns. Geoderma. 146(1–2), 192-200. http://dx.doi.org/10.1016/j.geoderma.2008.05.014.

Ding, F., Cai, J., Song, M., Yuan, P., 2013. The relationship between organic matter and specific surface area in <2 μm clay size fraction of muddy source rock. Sci. China Earth Sci. 56(8), 1343-1349. http://dx.doi.org/10.1007/s11430-013-4606-5

Faimon, J., Licbinska, M., Zajicek, P., 2012. Relationship between carbon dioxide in Balcarka Cave and adjacent soils in the Moravian Karst region of the Czech Republic. Int. J. Spel. 41(1), 17-28. http://dx.doi.org/10.5038/1827-806X.41.1.3.

Fang, C., Moncrieff, J.B., 1998. Simple and fast technique to measure CO_2 profiles in soil. Soil Biol. Biochem. 30(14), 2107-2112. http://dx.doi.org/10.1016/s0038-0717(98)00088-1.

Faybishenko, B.A., 1995. Hydraulic behavior of quasi-saturated soils in the presence of entrapped air: laboratory experiments. Water Resour. Res. 31(10), 2421-2435. http://dx.doi.org/10.1029/95WR01654.

Fernandez-Cortes, A., Cuezva, S., Garcia-Anton, E., Alvarez-Gallego, M., Pla, C., Benavente, D., Cañaveras, J.C., Calaforra, J.M., Mattey, D.P., Sanchez-Moral, S., 2015a. Changes in the storage and sink of carbon dioxide in subsurface atmospheres controlled by climate-driven processes: the case of the Ojo Guareña karst system. Environ. Earth Sci. 74, 7715–7730. http://dx.doi.org/10.1007/s12665-015-4710-2.

Fernandez-Cortes, A., Cuezva, S., Alvarez-Gallego, M., Garcia-Anton, E., Pla, C., Benavente, D., Jurado, V., Saiz-Jimenez, C., Sanchez-Moral, S., 2015b. Subterranean atmospheres may act as daily methane sinks. Nat. commun. 6, Article nº 7003. http://dx.doi.org/10.1038/ncomms8003.

Fusi, N., Martinez-Martinez, J., 2013. Mercury porosimetry as a tool for improving quality of micro-CT images in low porosity carbonate rocks. Eng. Geol. 166(0), 272-282. http://dx.doi.org/10.1016/j.enggeo.2013.10.002.

Gallage, C., Kodikara, J., Uchimura, T., 2013. Laboratory measurement of hydraulic conductivity functions of two unsaturated sandy soils during drying and wetting processes. Soils Found. 53(3), 417-430. http://dx.doi.org/10.1016/j.sandf.2013.04.004.

Galvan, S., Pla, C., Cueto, N., Martinez-Martinez, J., Garcia-del-Cura, M. A., Benavente, D., 2014. A comparison of experimental methods for measuring water permeability of porous building rocks. Materiales de Construcción 64, 315, e028. http://dx.doi.org/10.3989/mc.2014.06213.

Garcia-Anton, E., Cuezva, S., Fernandez-Cortes, A., Benavente, D., Sanchez-Moral, S., 2014a. Main drivers of diffusive and advective processes of CO_2-gas exchange between a shallow vadose zone and the atmosphere. Int. J. Greenh. Gas Control 21(0), 113-129. http://dx.doi.org/10.1016/j.ijggc.2013.12.006.

Garcia-Anton, E., Cuezva, S., Jurado, V., Porca, E., Miller, A.Z., Fernandez-Cortes, A., Saiz-Jimenez, C., Sanchez-Moral, S., 2014b. Combining stable isotope ($\delta^{13}C$) of trace gases and aerobiological data to monitor the entry and dispersion of microorganisms in caves. Environ. Sci. Pollut. R. 21(1), 473-484. http://dx.doi.org/10.1007/s11356-013-1915-3.

Hashimoto, S., Komatsu, H., 2006. Relationships between soil CO_2 concentration and CO_2 production, temperature, water content, and gas diffusivity: implications for field studies through sensitivity analyses. J For Res 11(1), 41-50. http://dx.doi.org/10.1007/s10310-005-0185-4.

Huang, H., Wu, P., Zhao, X., 2013. Effects of rainfall intensity, underlying surface and slope gradient on soil infiltration under simulated rainfall experiments. Catena 104, 93-102. http://dx.doi.org/10.1016/j.catena.2012.10.013.

Jabro, J.D., Sainju, U.M., Stevens, W.B., Evans, R.G., 2012. Estimation of CO_2 diffusion coefficient at 0-10 cm depth in undisturbed and tilled soils. Arch. Agron. Soil Sci. 58(1), 1-9. http://dx.doi.org/10.1080/03650340.2010.506482.

Jassal, R., Black, A., Novak, M., Morgenstern, K., Nesic, Z., Gaumont-Guay, D., 2005. Relationship between soil CO_2 concentrations and forest-floor CO_2 effluxes. Agric. For. Meteorol. 130(3-4), 176-192. http://dx.doi.org/10.1016/j.agrformet.2005.03.005.

Kaiser, K., Guggenberger, G., 2003. Mineral surfaces and soil organic matter. Eur. J. Soil Sci. 54(2), 219-236. http://dx.doi.org/10.1046/j.1365-2389.2003.00544.x

Keeling, C.D., 1958. The concentration and isotopic abundances of atmospheric carbon dioxide in rural areas. Geochim. Cosmochim. Ac. 13(4), 322-334. http://dx.doi.org/10.1016/0016-7037(58)90033-4.

Ketcham, R.A., Carlson, W.D., 2001. Acquisition, optimization and interpretation of X-ray computed tomographic imagery: applications to the geosciences. Comp. Geosci. 27, 381–400. http://dx.doi.org/10.1016/S0098-3004(00)00116-3.

Kowalczk, A.J., Froelich, P.N., 2010. Cave air ventilation and CO_2 outgassing by radon-222 monitoring: How fast do caves breathe? Earth Planet. Sci. Lett. 289, 209-219. http://dx.doi.org/10.1016/j.epsl.2009.11.010.

Kowalski, A.S., Serrano-Ortiz, P., Janssens, I.A., Sanchez-Moral, S., Cuezva, S., Domingo, F., Were, A., Alados-Arboledas, L., 2008. Can flux tower research neglect geochemical CO_2 exchange? Agric. For. Meteorol. 148, 1045–1054. http://dx.doi.org/10.1016/j.agrformet.2008.02.004.

Kuncoro, P.H., Koga, K., Satta, N., Muto, Y., 2014. A study on the effect of compaction on transport properties of soil gas and water I: Relative gas diffusivity, air permeability, and saturated hydraulic conductivity. Soil Tillage Res. 143, 172-179. http://dx.doi.org/10.1016/j.still.2014.02.006.

Kuzyakov, Y., 2006. Sources of CO_2 efflux from soil and review of partitioning methods. Soil Biol. Biochem. 38(3), 425-448. http://dx.doi.org/10.1016/j.soilbio.2005.08.020.

Leelamanie, D.A.L., 2014. Initial water repellency affected organic matter depletion rates of manure amended soils in Sri Lanka. J. Hydrol. Hydromechanics 62(4), 309-315. http://dx.doi.org/10.2478/johh-2014-0040.

Li, M., Shimizu, M., Hatano, R., 2015. Evaluation of N_2O and CO_2 hot moments in managed grassland and cornfield, southern Hokkaido, Japan. Catena. 133, 1-13. http://dx.doi.org/10.1016/j.catena.2015.04.014.

Loisy, C., Cohen, G., Laveuf, C., Le Roux, O., Delaplace, P., Magnier, C., Rouchon, V., Cerepi, V., Garcia, B., 2013. The CO_2-Vadose Project: Dynamics of the natural CO_2 in a carbonate vadose zone. Int. J. Greenh. Gas Control 14, 97-112. http://dx.doi.org/10.1016/j.ijggc.2012.12.017.

Menon, M., Jia, X., Lair, G.J., Faraj, P.H., Blaud, A., 2015. Analysing the impact of compaction of soil aggregates using X-ray microtomography and water flow simulations. Soil Tillage Res. 150(0), 147-157. http://dx.doi.org/10.1016/j.still.2015.02.004.

Millington, R.J., Quirk, J.P., 1960. Transport in porous media. In: Van Baren, F.A. (Ed), Transactions of the 7th International Congress of Soil Science, vol. 1. Elsevier, Amsterdam, pp. 97–106.

Millington, R.J., Quirk, J.P., 1961. Permeability of porous solids. Trans. Faraday Soc. 57(8), 1200-1207. http://dx.doi.org/10.1039/tf9615701200.

Moitinho, M.R., Padovan, M.P., Panosso, A.R., Teixeira, D.D.B., Ferraudo, A.S., La Scala, Jr. N., 2015. On the spatial and temporal dependence of CO_2 emission on soil properties in sugarcane (Saccharum spp.) production. Soil Tillage Res. 148(0), 127-132. http://dx.doi.org/10.1016/j.still.2014.12.012.

Moldrup, P., Kruse, C.W., Yamaguchi, T., Rolston, D.E., 1996. Modeling diffusion and reaction in soils. 1. A diffusion and reaction corrected finite difference calculation scheme. Soil Sci. 161(6), 347-354. http://dx.doi.org/10.1097/00010694-199606000-00001.

Neris, J., Jimenez, C., Fuentes, J., Morillas, G., Tejedor, M., 2012. Vegetation and land-use effects on soil properties and water infiltration of Andisols in Tenerife (Canary Islands, Spain). Catena 98, 55-62. http://dx.doi.org/10.1016/j.catena.2012.06.006.

Neris, J., Tejedor, M., Rodríguez, M., Fuentes, J., Jimenez, C., 2013. Effect of forest floor characteristics on water repellency, infiltration, runoff and soil loss in Andisols of Tenerife (Canary Islands, Spain). Catena 108(0), 50-57. http://dx.doi.org/10.1016/j.catena.2012.04.011.

Penman, H.L., 1940. Gas and vapour movements in the soil II. The diffusion of carbon dioxide through porous solids. J. Agric. Sci. 30, 570-581.

Phillips, C.L., Nickerson, N., Risk, D., Bond, B.J., 2011. Interpreting diel hysteresis between soil respiration and temperature. Global Change Biol. 17(1), 515-527. http://dx.doi.org/10.1111/j.1365-2486.2010.02250.x.

Pingintha, N., Leclerc, M.Y., Beasley Jr, J.P., Zhang, G., Senthong, C., 2010. Assessment of the soil CO_2 gradient method for soil CO_2 efflux measurements: comparison of six models in the calculation of the relative gas diffusion coefficient. Tellus B. 62(1), 47-58. http://dx.doi.org/10.1111/j.1600-0889.2009.00445.x.

Pla, C., Galiana-Merino, J.J., Cuezva, S., Fernandez-Cortes, A., Garcia-Anton, E., Cuevas-Gonzalez, J., Cañaveras, J.C., Sanchez-Moral, S., Benavente, D., 2014. Environmental factors controlling transient and seasonal changes of trace gases within shallow vadose zone. In EGU General Assembly Conference Abstracts, vol. 16, p. 8410.

Pla, C., Galiana-Merino, J.J., Cuevas-Gonzalez, J., Andreu, J.M., Cañaveras, J.C., Cuezva, S., Fernandez-Cortes, A., Garcia-Anton, E., Sanchez-Moral, S., Benavente, D., 2015. Definition of microclimatic conditions in a karst cavity: Rull Cave (Alicante, Spain). In Andreo, B., Carrasco, F., Duran, J.J., Jimenez, P., La Moreaux, J.W. (Eds.), Hydrogeological and Environmental Investigations in Karst Systems, vol. 1. Springer Berlin Heidelberg, pp. 497-503. http://dx.doi.org/10.1007/978-3-642-17435-3_56.

Pla, C., Cuezva, S., Garcia-Anton, E., Fernandez-Cortes, A., Cañaveras, J.C., Sanchez-Moral, S., Benavente, D., 2016a. Changes in the CO_2 dynamics in near-surface cavities under a future warming scenario: Factors and evidence from the field and experimental findings. Sci. Total Environ. 565, 1151-1164. http://dx.doi.org/10.1016/j.scitotenv.2016.05.160.

Pla, C., Galiana-Merino, J.J., Cuezva, S., Fernandez-Cortes, A., Cañaveras, J.C., Benavente, D., 2016b. Assessment of CO_2 dynamics in subsurface atmospheres using thewavelet approach: from cavity atmosphere exchange to anthropogenic impacts in Rull cave (Vall d'Ebo, Spain). Environ. Earth Sci. 75(5), 446. http://dx.doi.org/10.1007/s12665-016-5325-y.

Ridgwell, A.J., Marshall, S.J., Gregson, K., 1999. Consumption of atmospheric methane by soils: A process-based model. Global Biogeochem. Cycles. 13, 59–70. http://dx.doi.org/10.1029/1998GB900004.

Rivas-Martinez, S., 1983. Pisos bioclimáticos de España. Lazaroa 5, 33–44.

Roduit, N. JMicroVision: Image analysis toolbox for measuring and quantifying components of high-definition images. Version 1.2.7. http://www.jmicrovision.com (accessed 15 September 2015).

Rolston, D.E., Møldrup, P., 2002. Methods of Soil Analysis, Part 4: Physical Methods. Eds. Dane, J.H., Topp, G.C. Madison.

Rouquerol, J., Avnir, D., Fairbridge, C.W., Everett, D.H., Haynes, J.H., Pernicone, N., Ramsay, J.D.F., Sing, K.S.W., Unger, K.K., 1994. Recommendations for the characterization of porous solids. Pure Appl. Chem. 66, 1739-1758.

Saiz-Jimenez, C., Cuezva, S., Jurado, V., Fernandez-Cortes, A. Porca, E., Benavente, D., Cañaveras, J.C., Sanchez-Moral, S., 2011. Paleolithic art in peril: Policy and science collide at altamira cave. Science 334(6052), 42-43. http://dx.doi.org/10.1126/science.1206788.

Sanchez-Moral, S., Soler, V., Cañaveras, J.C., Sanz-Rubio, E., Van Grieken, R., Gysels, K., 1999. Inorganic deterioration affecting the Altamira Cave, N Spain: Quantitative approach to wall-corrosion (solutional etching) processes induced by visitors. Sci. Total Environ. 243-244, 67-84. http://dx.doi.org/10.1016/S0048-9697(99)00348-4.

Sanchez-Moral, S., Cuezva, S., Fernandez-Cortes, A., Benavente, D., Cañaveras, J.C., 2010. Effect of ventilation on karst system equilibrium (Altamira cave, N Spain): An appraisal of karst contribution to the global carbon cycle balance. In: Andreo, B., Carrasco, F., Duran, J.J., La Moreaux, J.W. (Eds.), Advances in Research in Karst Media. Springer-Verlag Berlin Heidelberg, pp. 469-474. http://dx.doi.org/10.1007/978-3-642-12486-0_72.

Sanci, R., Panarello, H.O., Ostera, H.A., 2009. Assessment of soil moisture influence on CO_2 flux: a laboratory experiment. Environ. Geol. 58(3), 491-497. http://dx.doi.org/10.1007/s00254-008-1522-7.

Schlesinger, W.H., Andrews, J.A., 2000. Soil respiration and the global carbon cycle. Biogeochemistry 48, 7–20. http://dx.doi.org/10.1023/A:1006247623877.

Schön, J., 2011. Physical properties of rocks: A workbook, vol. 8. Elsevier.

Serrano-Ortiz, P., Roland, M., Sanchez-Moral, S., Janssens, I.A., Domingo, F., Godderis, Y., Kowalski, A.S., 2010. Hidden, abiotic CO_2 flows and gaseous reservoirs in the terrestrial carbon cycle: review and perspectives. Agric. For. Meteorol. 150, 321–329. http://dx.doi.org/10.1016/j.agrformet.2010.01.002.

Shahraeeni, E., Or, D., 2012. Pore scale mechanisms for enhanced vapor transport through partially saturated porous media. Water Resour. Res. 48(5). http://dx.doi.org/10.1029/2011WR011036.

Tang, J.W., Baldocchi, D.D., Qi, Y., Xu, L.K., 2003. Assessing soil CO_2 efflux using continuous measurements of CO2 profiles in soils with small solid-state sensors. Agric. For. Meteorol. 118(3-4), 207-220. http://dx.doi.org/10.1016/s0168-1923(03)00112-6.

Tiab, D., Donaldson, E.C., 1996. Petrophysics: theory and practice of measuring reservoir rock and fluid transport properties. Gulf Publishing Company, Houston, Texas.

Troeh, F.R., Jabro, J.D., Kirkham, D., 1982. Gaseous-diffusion equations for porous materials. Geoderma. 27(3), 239-253. http://dx.doi.org/10.1016/0016-7061(82)90033-7.

Turcu, V.E., Jones, S.B., Or, D., 2005. Continuous soil carbon dioxide and oxygen measurements and estimation of gradient-based gaseous flux. Vadose Zone J. 4(4), 1161-1169. http://dx.doi.org/10.2136/vzj2004.0164.

Vogelmann, E.S., Reichert, J.M., Prevedello, J., Consensa, C.O.B., Oliveira, A.E., Awe, G.O., Mataix-Solera, J., 2013. Threshold water content beyond which hydrophobic soils become hydrophilic: The role of soil texture and organic matter content. Geoderma 209-210, 177-187. http://dx.doi.org/10.1016/j.geoderma.2013.06.019.

Xu, L., Baldocchi, D.D., Tang, J., 2004. How soil moisture, rain pulses, and growth alter the response of ecosystem respiration to temperature. Global Biogeochem. Cycles 18(4). http://dx.doi.org/10.1029/2004GB002281.

Xu, X., Luo, X., 2012. Effect of wetting intensity on soil GHG fluxes and microbial biomass under a temperate forest floor during dry season. Geoderma 170, 118-126. http://dx.doi.org/10.1016/j.geoderma.2011.11.016.

Zhang, Z.H., Ouriadov, A.V., Willson, C., Balcom, B.J., 2005. Membrane gas diffusion measurements with MRI. J Magn. Reson. 176(2), 215-222. http://dx.doi.org/10.1016/j.jmr.2005.06.009.

Zhang, J., Sequaris, J.M., Klumpp, E., 2013. Effects of natural organic matter on the microporous sorption sites of black carbon in a Yangtze River sediment. Environ. Sci. Pollut. R. 20(10), 6992-6998. http://dx.doi.org/10.1007/s11356-013-1712-z.

Zongping, R., Liangjun, Z., Bing, W., Shengdong, C., 2016. Soil hydraulic conductivity as affected by vegetation restoration age on the Loess Plateau, China. J. Arid Land 8(4), 546-555. http://dx.doi.org/10.1007/s40333-016-0010-2.

Tables

Table 1. Physical properties of the studied soils (Altamira and Rull).

Soil sample	Grain density ($g\ cm^{-3}$)	Bulk density ($g\ cm^{-3}$)	Total porosity (-)	Air filled porosity (-)	Specific surface area ($m^2\ g^{-1}$)	Hydraulic conductivity ($m\ s^{-1}$)	Organic matter (%)
Altamira	2.50	1.30	0.48	0.23	7.42	$4.84 \cdot 10^{-7}$	9.4
Rull	2.36	1.13	0.52	0.34	11.36	$3.49 \cdot 10^{-7}$	14.7

Table 2. CO_2 diffusion coefficients determined for the different soil samples.

Sample	Calculated CO_2 diffusion coefficient **$(m^2\ s^{-1}) \cdot 10^{-6}$**	
	Altamira	Rull
Dry soil (0%)	4.02	1.49
Compacted dry soil (0%)	3.50	1.00
Wet soil (30%)	0.54	0.61
Wet soil (62%)	0.32	0.32

Tables

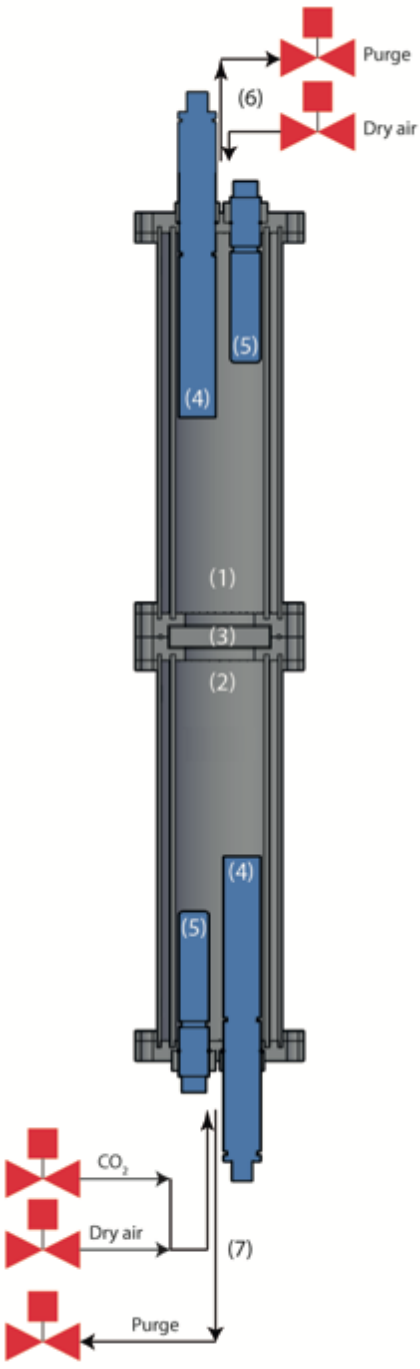

Figure 1. Laboratory device designed to measure gas diffusion. (1) Top chamber. (2) Bottom chamber. (3) Sample. (4) CO_2 concentration probe and (5) temperature and relative humidity probes in the top and bottom chamber. (6, 7) Set of valves in the top and bottom chamber.

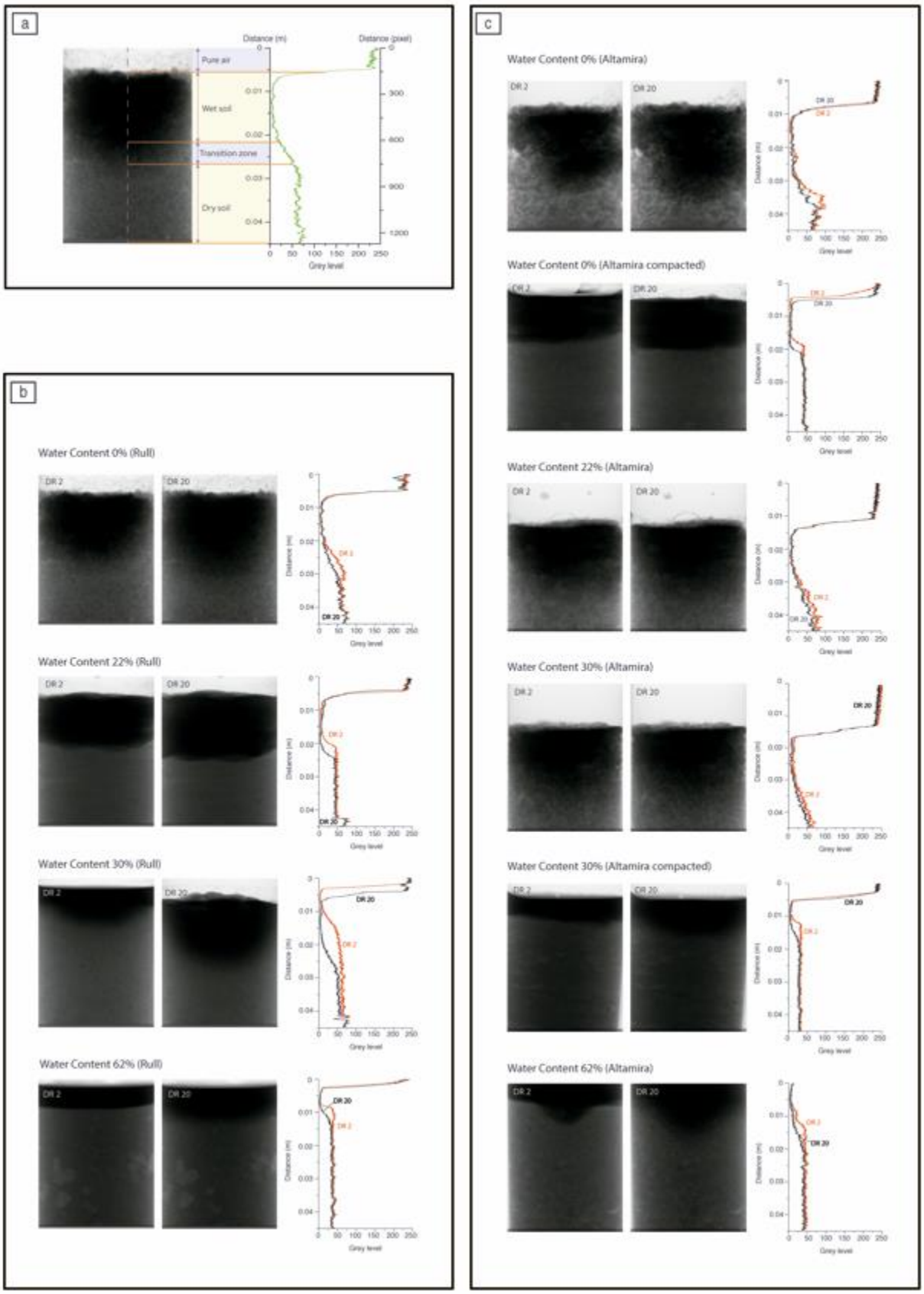

Figure 2. (a) Example of a vertical grey level profile obtained from a radiography after performing digital image analysis. (b) Water front advance for radiographies 2 and 20 for Rull samples and (c) Altamira samples.

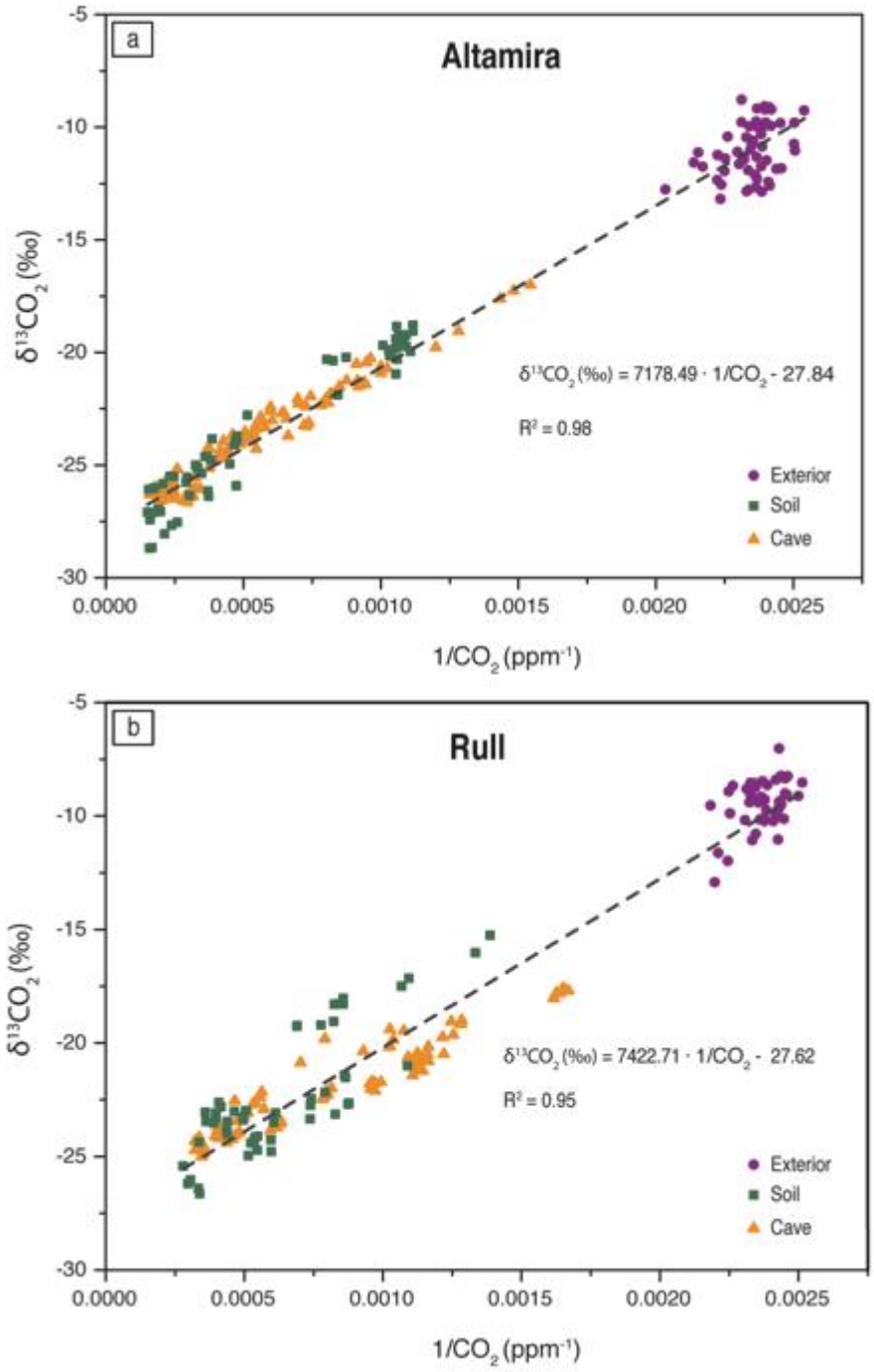

Figure 3. (a) Keeling plot for the discrete sampling in Altamira in soil, exterior and inside the cavity. (b) Keeling plot for the discrete sampling in Rull soil, exterior and cave air.

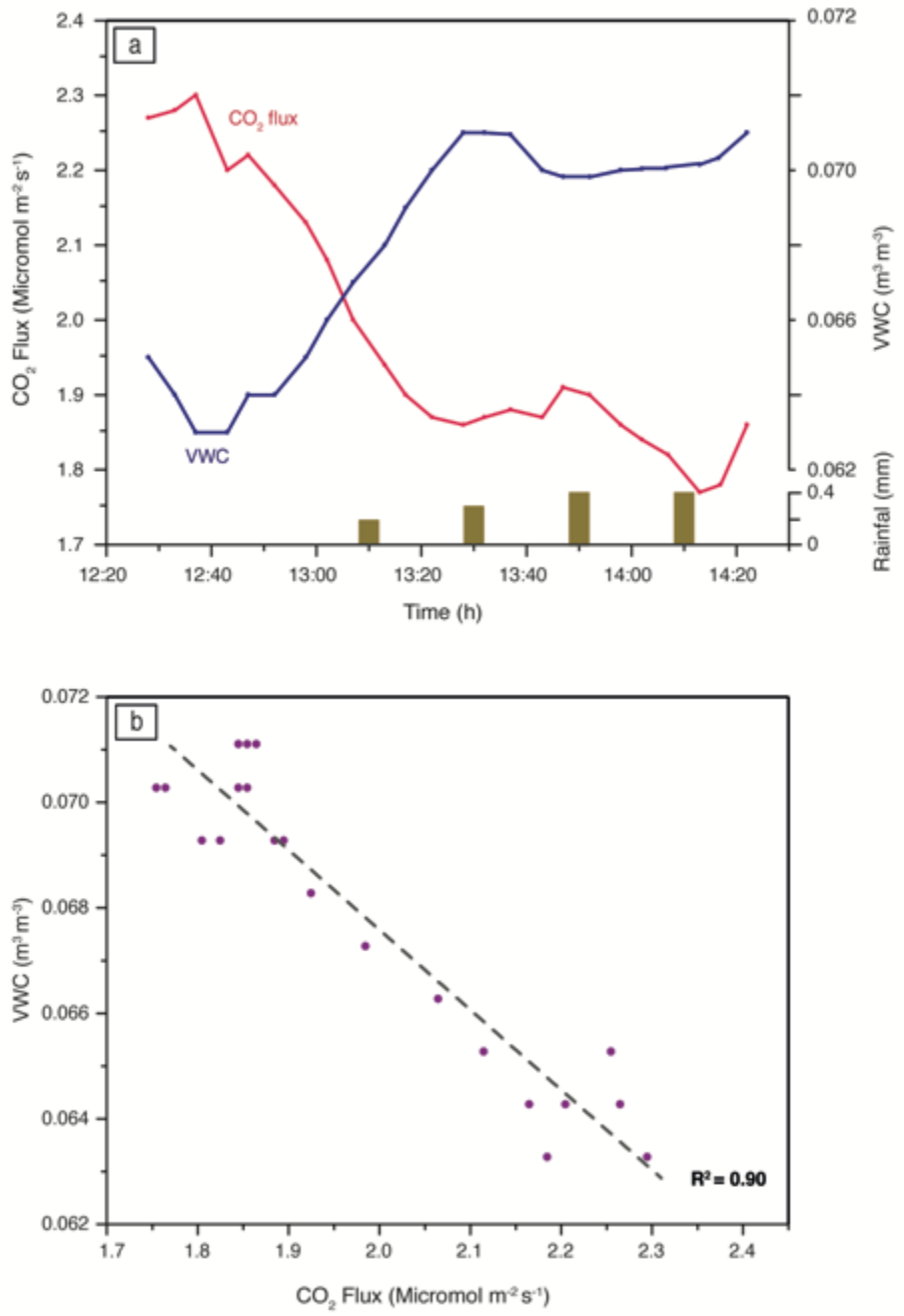

Figure 4. (a) Rainfall and CO_2 fluxes and VWC in soil above Rull cave (January 13, 2014). (b) Linear regression analysis between CO_2 flux and VWC.

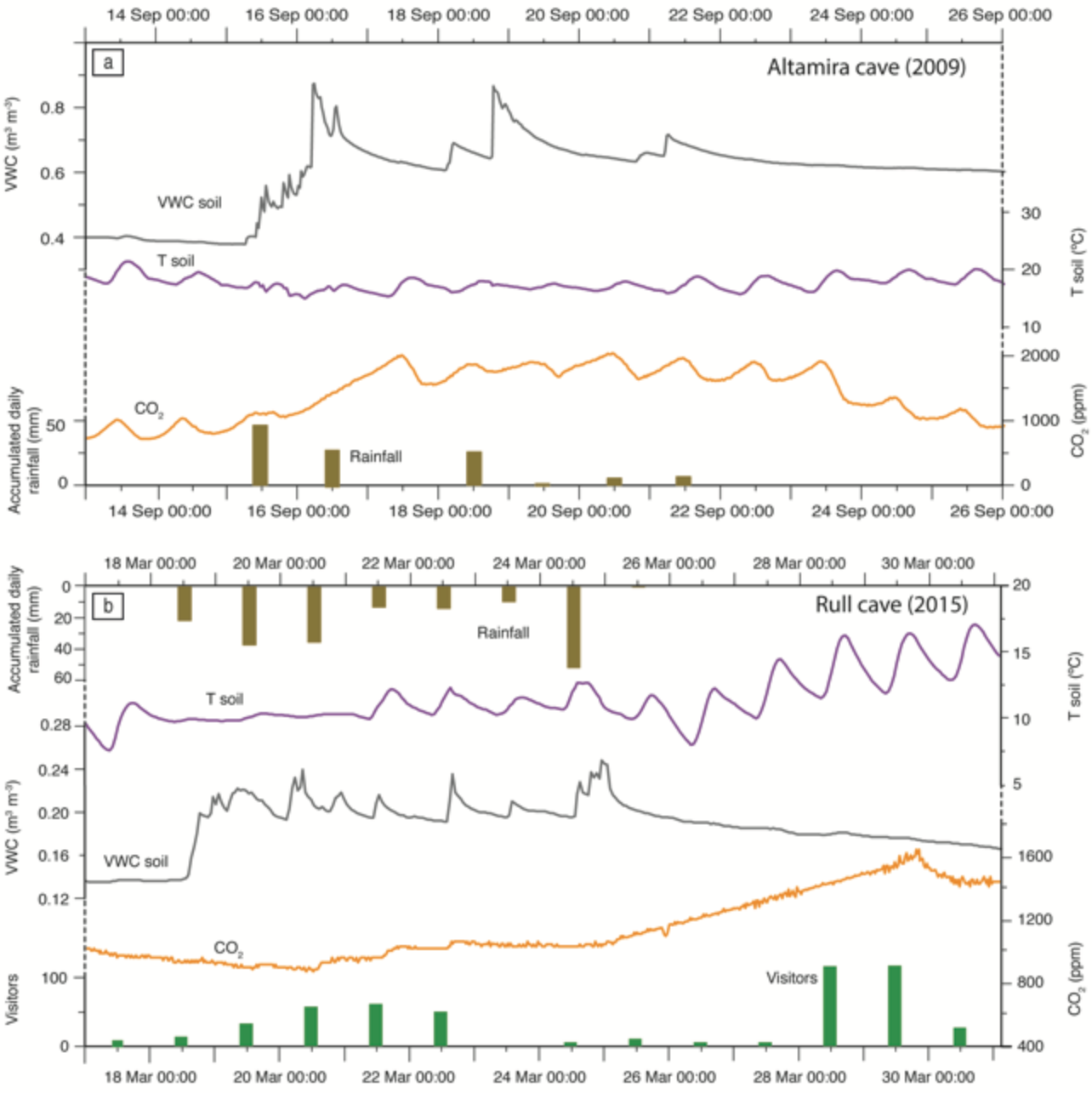

Figure 5. Soil and cave conditions registered during the studied events in Altamira (a) and Rull (b) caves.

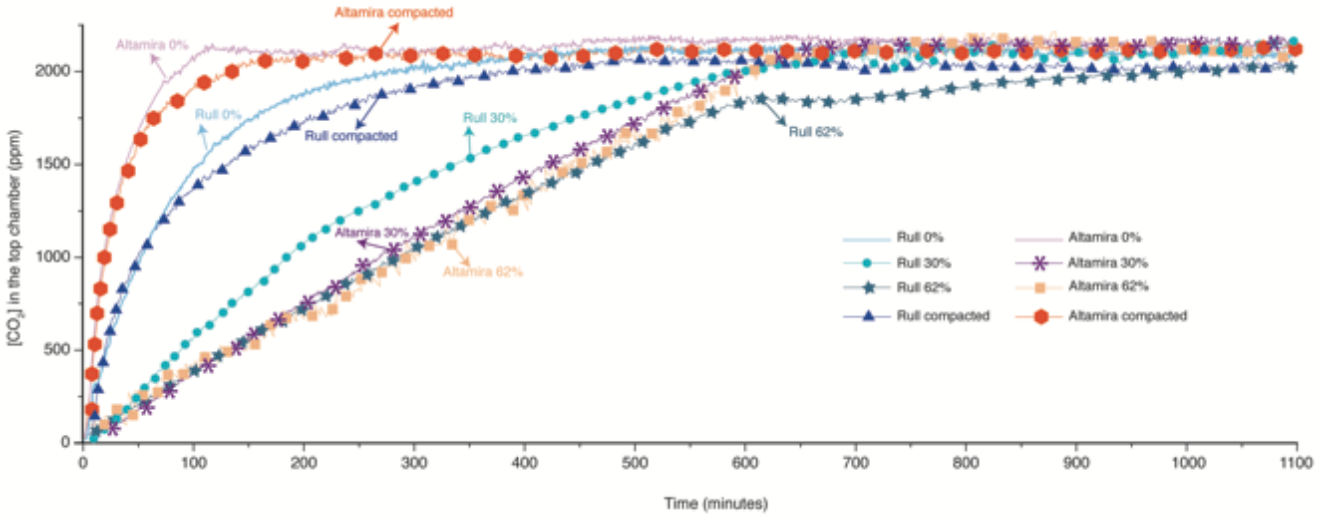

Figure 6. Variations in CO_2 diffusion coefficients for the different compaction degrees and water contents in soils.

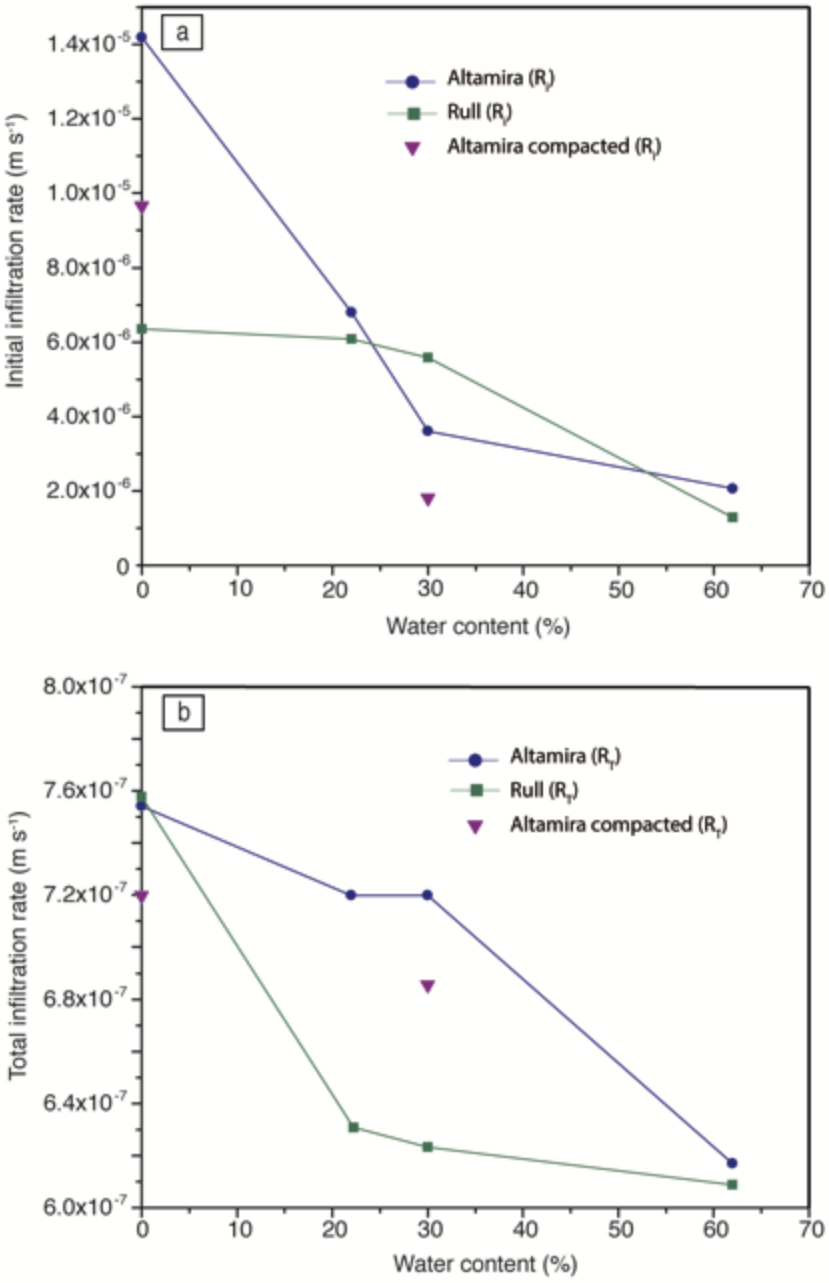

Figure 7. (a) Initial infiltration rates (R_i) for the different samples. (b) Total infiltration rates (R_T) for the different samples.

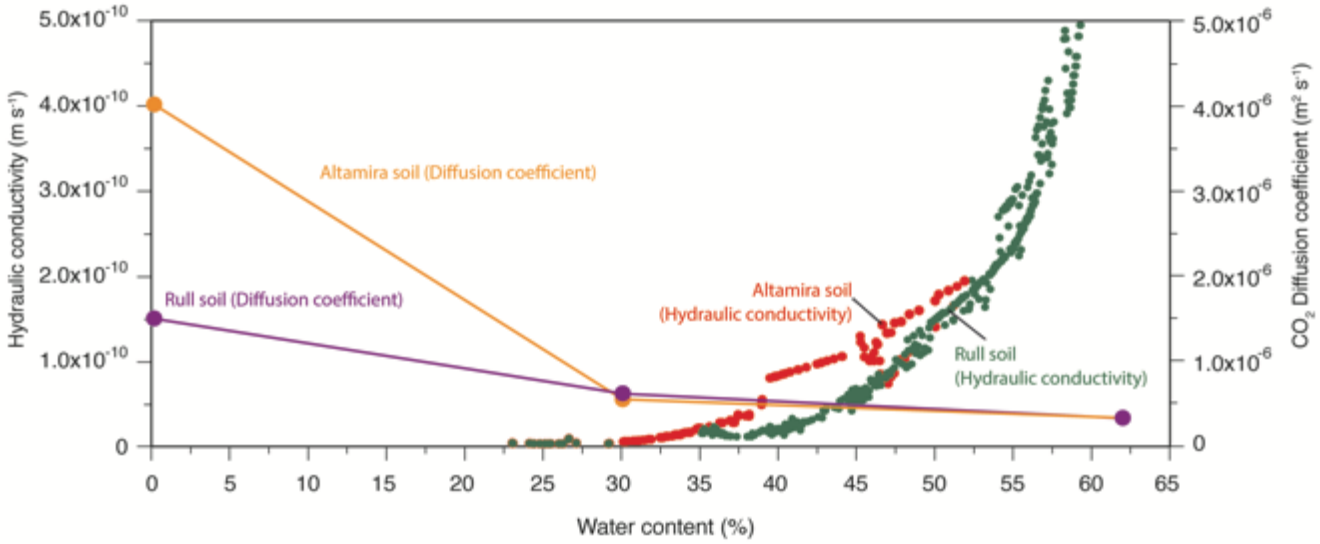

Figure 8. Data of relative hydraulic conductivity functions for the both soils, obtained from ku-pF experiment and CO_2 diffusion coefficients for different soil water contents.

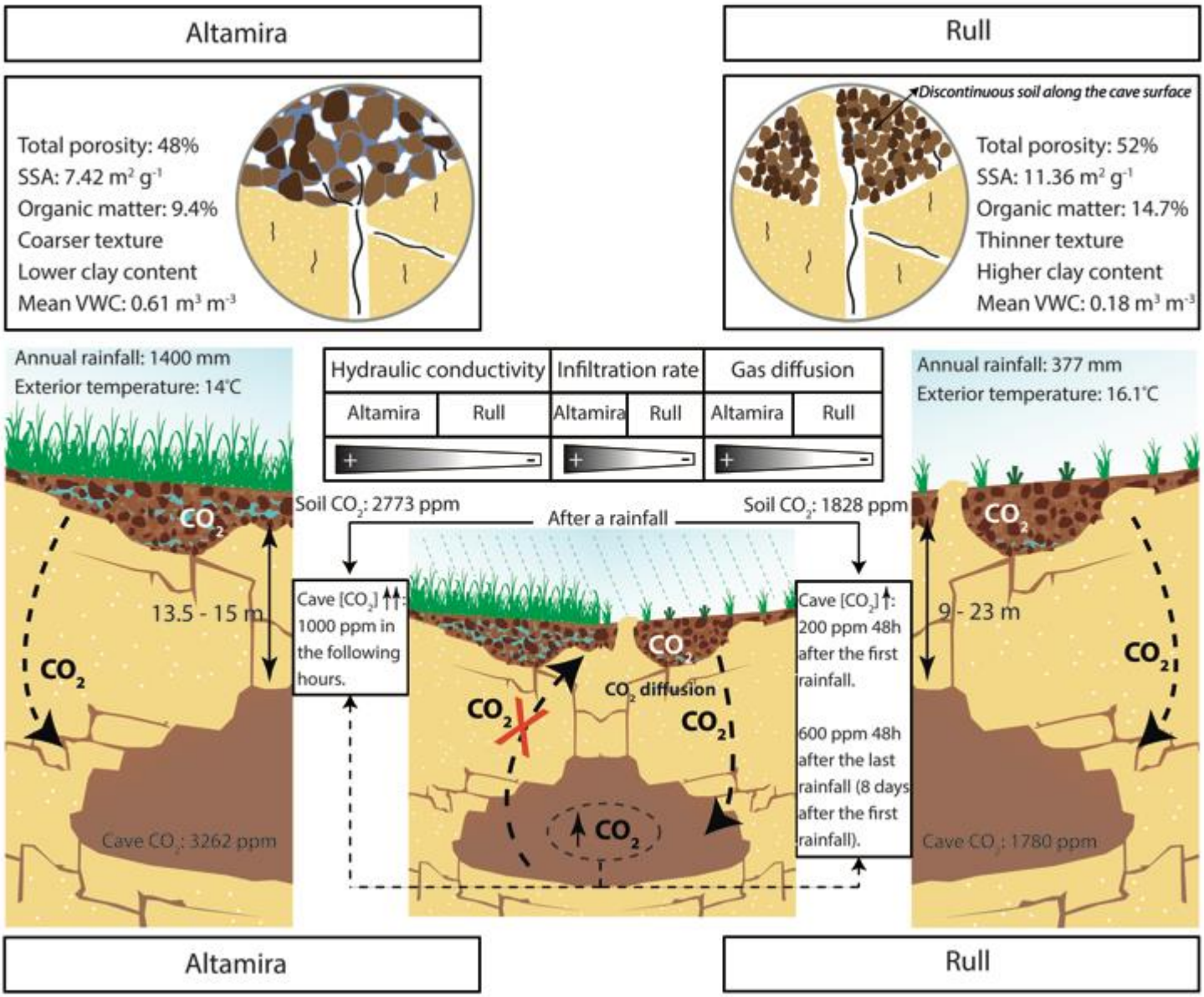

Figure 9. Synthesis of both field sites (Rull and Altamira). The figure highlights the differences between the both scenarios and the different evolution after a rainfall event. Soil properties are also remarked. Values of volumetric water content in soil (VWC), exterior temperature and CO_2 concentration in soil and caves are annual averaged values.